Supporting Information for:

Fluorophore Incorporation Allows Nanomolar Guest Sensing and White-Light Emission in M_4L_6 Cage Complexes

Prakash P. Neelakandan, Azucena Jiménez, and Jonathan R. Nitschke*

Department of Chemistry, University of Cambridge, Lensfield Road, Cambridge CB2 1EW, United Kingdom

Experimental Section

General experimental techniques: All reagents and solvents were purchased from commercial sources and used as supplied. All experiments were carried out at room temperature. Spectroscopy grade acetonitrile was used for UV-Vis absorption and fluorescence measurements and was distilled prior to use. Microwave reactions were performed with a CEM Discover microwave reactor. NMR spectra were recorded using either a Bruker DRX-400, a Bruker AVC-500-BB or a Bruker AVC-500-TCI spectrometer. Chemical shifts are reported in parts per million (δ) calibrated to the residual solvent signals: δ_H with [D_3]acetonitrile at 1.940 ppm and δ_C with [D_3]acetonitrile at 118.260 ppm.[19]F NMR values are calibrated to the internal standard hexafluorobenzene (–164.90 ppm) or the counter anions triflate (–79.5 ppm) or triflimide (–80.4 ppm).[1] High resolution mass spectrometry was performed on a Waters LCT Premier Mass Spectrometer featuring a Z-spray source with electrospray ionization and modular LockSpray interface. Molecular modelling was done using the modified MM2 force field of CAChe Workspace, WorkSystem Pro Version 7.5.0.85. UV-Vis absorption measurements were performed on a Perkin-Elmer Lambda 750 spectrometer. Fluorescence measurements were performed on a Cary Eclipse fluorescence spectrophotometer. Rhodamine 110 in basic ethanol (Φ_F = 0.92) or quinine sulphate in 1 N H_2SO_4 (Φ_F = 0.55) were used as the standards.[2] Quantum yields of fluorescence were calculated using the equation 1,

$$\Phi_u = \frac{A_s F_u n_u^2}{A_u F_s n_s^2} \Phi_s \qquad (1)$$

where Φ represents the fluorescence quantum yield, A the absorbance, F the areas of fluorescence peaks and n the refractive index of the solvent used. The subscripts "s" and "u" denote these parameters for the standard and unknown compounds, respectively.

Synthesis

Synthesis of bis(aminophenyl)BODIPY **1**

The bis(nitrophenyl)BODIPY **9** (Scheme S1) was synthesized as reported elsewhere.[3-5] A solution of the bis(nitrophenyl)BODIPY **9** (100 mg, 0.18 mmol) in methanol (20 mL) was stirred at room temperature followed by the addition of 10 % Pd/C (15.0 mg). The reaction mixture was degassed and stirred at room temperature for 5 h under an atmosphere of dihydrogen. The solution was filtered through Celite, concentrated in vacuo, and purified *via* flash column chromatography over silica gel using dichloromethane as eluent followed by ethyl acetate to yield **1** as a dark green powder (86 mg, 97 %). ^{1}H NMR (400 MHz, CD_3CN): δ = 2.12 (s, 6H), 2.38 (s, 3H), 4.27 (s, 4H), 6.61 (d, J = 8 Hz, 4H), 6.70 (s, 2H), 7.06 (s, 2H), 7.32 (d, J = 8.0 Hz, 4H), 8.26 (s, 2H); ^{13}C NMR (100 MHz, CD_3CN): δ = 20.0, 21.2, 115. 5, 122.3, 127.5, 129.0, 130.7, 135.8, 137.0, 137.3, 139.8, 142.5, 145.7, 148.8; ^{19}F NMR (376 MHz, CD_3CN): δ = –147.8 to –148.1 (m, 2F); HRMS (ESI): *m/z*: calculated for $C_{30}H_{27}N_4BF_2$ $[M–H]^+$: 493.2370, found: 493.2351.

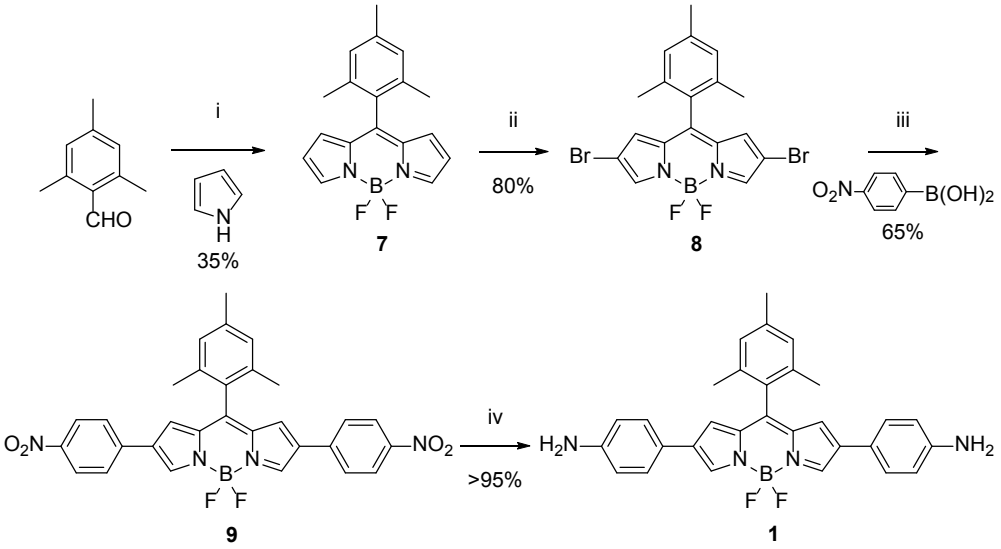

Scheme S1. Synthesis of subcomponent **1**. (i) (a) TFA, 5 min; (b) toluene, DDQ, RT, 2 h; (c) DCM, TEA, $BF_3{\cdot}OEt_2$, RT, 30 min, 35 %; (ii) NBS, 1:1 DCM:DMF, 25 °C, 8 h, 80 %; (iii) 4-nitrophenylboronic acid, $Pd_2(dba)_3{\cdot}CHCl_3$, tBu$_3$P·HBF$_4$, Cs_2CO_3, THF : water, 25 °C, 24 h, 65 %; (iv) H_2/Pd-C, MeOH, 25 °C, 5 h, 95 %.

Synthesis of 5-(pyren-1-yl)picolinaldehyde (**2**)

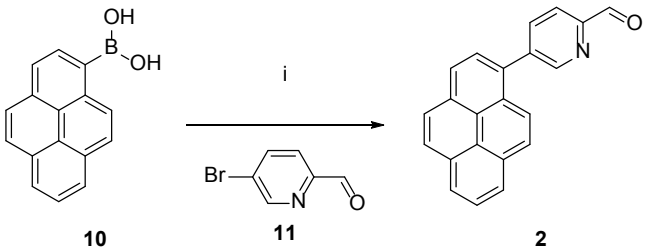

Scheme S2. Synthesis of subcomponent **2**. (i) $Pd(PPh_3)_4$, aq. NaOH (1 M), toluene, 100 °C, 30 min, 200 W microwave, 65 %.

As shown in Scheme S2, the coupling between pyren-1-ylboronic acid (**10**) and 5-bromopicolinaldehyde (**11**) under Suzuki conditions yielded the pyrene appended 2-formylpyridine (**2**). In a vial suitable for microwave reactions, pyrene-1-boronic acid (**10**, 160 mg, 0.65 mmol), 5-bromo-2-formylpyridine (**11**, 100 mg, 0.54 mmol), and tetrakis(triphenylphosphine)palladium(0) (6.2 mg, 0.0054 mmol) were suspended in a mixture of toluene (8 mL) and 1 M aqueous NaOH solution (4 mL). The vial was flushed with nitrogen, capped, and heated in the microwave reactor at 100 °C for 30 minutes at 200 W. The reaction mixture was cooled down to room temperature, washed with water (3 × 20 mL), dried over $MgSO_4$ and concentrated in vacuo to yield a dark yellow residue. The product was isolated by column chromatography over silica gel using dichloromethane as eluent to yield **2** as yellow crystals (108 mg, 65 %). ^{1}H NMR (400 MHz, CD_3CN): δ = 8.20 (m, 11H), 9.06 (s, 1H), 10.16 (s, 1H); ^{13}C NMR (100 MHz, CD_3CN): δ = 122.2, 125.0, 125.2, 125.5, 125.9, 126.4, 126.8, 127.6, 128.3, 128.7, 129.1, 129.38, 129.44, 131.7, 132.3, 132.5, 133.5, 139.9, 141.9, 152.4, 152.6, 194.4; HRMS (ESI): *m/z*: calculated for $C_{22}H_{13}NO$ $[M–H]^+$ 308.1070, found: 308.1073.

General procedure for the preparation of cages: In a Teflon-capped J-Young NMR tube, **1** (0.0203 mmol), either **2** or **3** (0.0406 mmol), and either $Fe^{II}(OTf)_2$ (0.0136 mmol) or $Zn^{II}(NTf_2)_2$ (0.0136 mmol) were dissolved in CD_3CN (0.5 mL). The solution was degassed by three evacuation/nitrogen-fill cycles and heated at 70 °C overnight. After cooling down to room temperature, the solvent was removed and the residue was washed with diethyl ether to yield the self-assembled structures.

4: ^{1}H NMR (400 MHz, CD_3CN): δ = 2.14 to 2.19 (36H, m), 2.41 to 2.47 (18H, m), 5.27 to 5.33 (24H, m), 7.00 to 7.38 (36H, m), 7.46 to 7.55 (24H, m), 7.69 to 7.73 (12H, m), 8.32 to 8.47 (24H, m), 8.57 to 8.64 (12H, m), 8.71 to 8.78 (12H, m); ^{13}C NMR (100 MHz, CD_3CN): δ = 19.8 to 19.9, 20.8 to 21.1, 122.3 to 122.6, 125.1 to 125.5, 126.8 to 127.4, 128.8 to 129.1, 129.8 to 129.9, 130.2 to 130.3, 131.5 to 131.7, 133.0 to 133.8, 136.8 to 137.1, 140.0 to 140.2, 143.2 to 143.4, 143.8 to 144.1, 144.5, 148.3, 149.6 to 150.0, 156.4, 158.9, 175.1 to 175.4; ^{19}F NMR (376 MHz, CD_3CN): δ = –79.5 (OTf), –143.2 to –144.1, –144.3 to –144.8, –145.5 to –145.8, –146.4 to –146.9,–147.9 to –148.5.

5: ^{1}H NMR (400 MHz, CD_3CN): δ = 2.22 to 2.30 (36H, m), 2.40 to 2.45 (18H, m), 5.71 to 5.76 (24H, m), 7.03 to 8.48 (180H, m), 8.72 to 8.90 (24H, m), 9.05 to 9.13 (12H); ^{13}C NMR (100 MHz, CD_3CN): δ = 20.1 to 20.3, 21.1 to 21.2, 122.8 to 123.6, 124.6, 125.1, 125.8, 126.3 to 126.5, 127.1 to 127.3, 127.5, 128.0, 129.2 to 129.3, 129.6, 129.6, 130.1, 130.8, 131.9, 130.8, 131.9, 132.8, 133.5, 137.1 to 137.5, 140.4, 141.5 to 141.7, 142.8, 143.6, 148.7, 157.2 to 157.3, 157.6 to 157.8, 175.4 to 175.7; ^{19}F NMR (376 MHz, CD_3CN): δ = –79.5 (OTf), –142.7 to –144.3, –145.1 to –145.3, –146.0 to –146.5,–147.4 to –148.0.

6: ^{1}H NMR (400 MHz, CD_3CN): δ = 2.08 to 2.19 (36H, m), 2.35 to 2.46 (18H, m), 6.06 to 6.27 (24H, m), 6.97 to 7.20 (24H, m), 7.50 to 7.57 (24H, m), 7.82 to 7.98 (24H, m), 8.07 to

8.21 (12H, m), 8.39 to 8.60 (36H, m); ^{19}F NMR (376 MHz, CD_3CN): δ = –80.5 (NTf_2), –143.4 to –144.8, –145.1 to –146.1, –146.7 to –147.5.

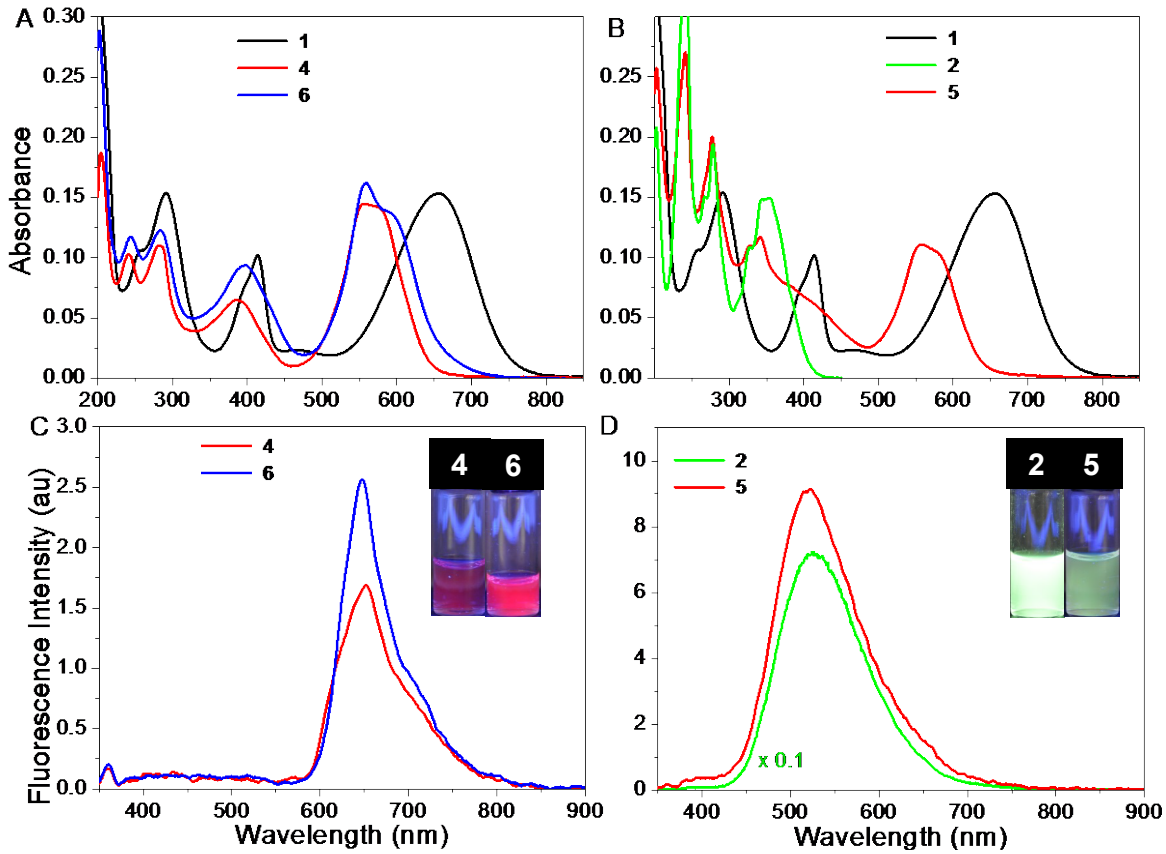

Figure S1. (A, B) UV-Vis absorption and (C, D) fluorescence spectra of the subcomponents **1** (3.5 µM) and **2** (5 µM) and the metallo-supramolecular cages **4** (65 nM), **5** (110 µM), and **6** (75 nm) in acetonitrile, λ_{ex} = 326 nm. Insets show the fluorescence of **4**, **6**, **2** and **5** in acetonitrile illuminated with a hand held UV lamp.

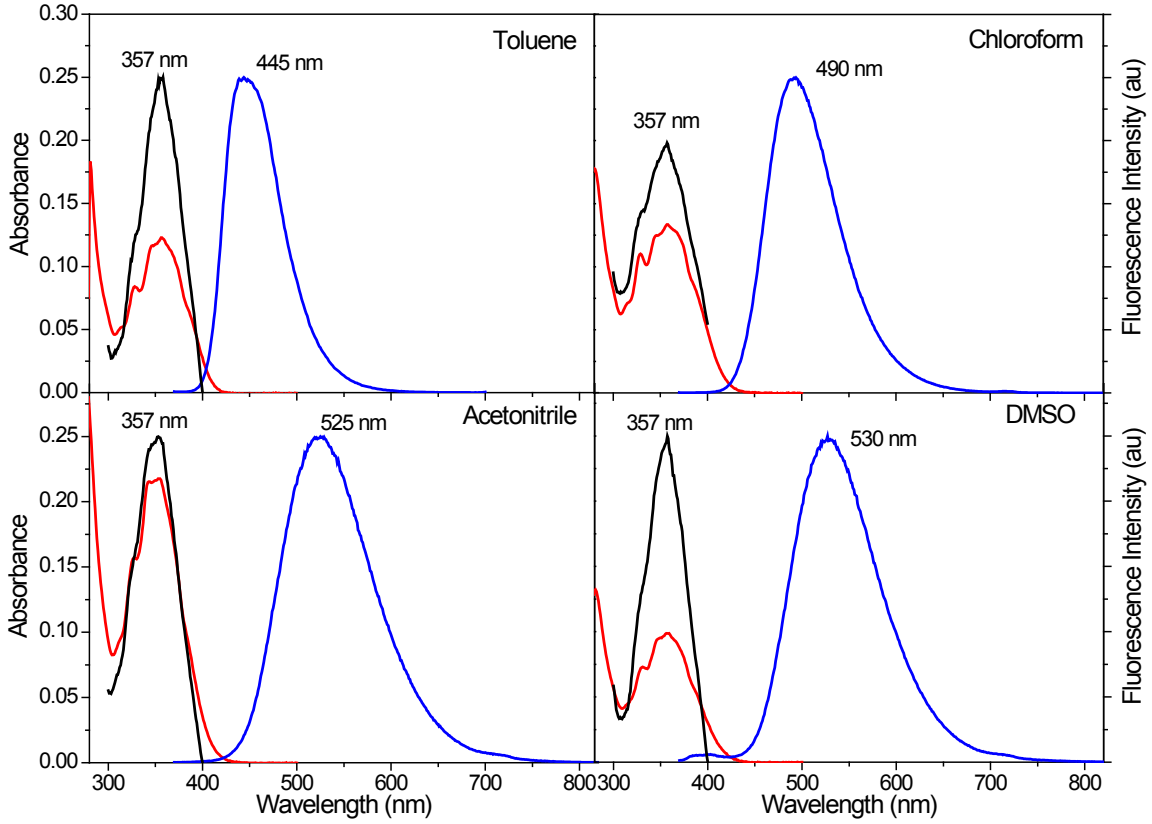

Figure S2. UV-Vis absorption (red), fluorescence emission (blue) and fluorescence excitation (black) spectra of the subcomponent **2** (4 to 7 μM) in various solvents, λ_{ex} = 357 nm. Excitation spectra were collected at the respective emission maxima.

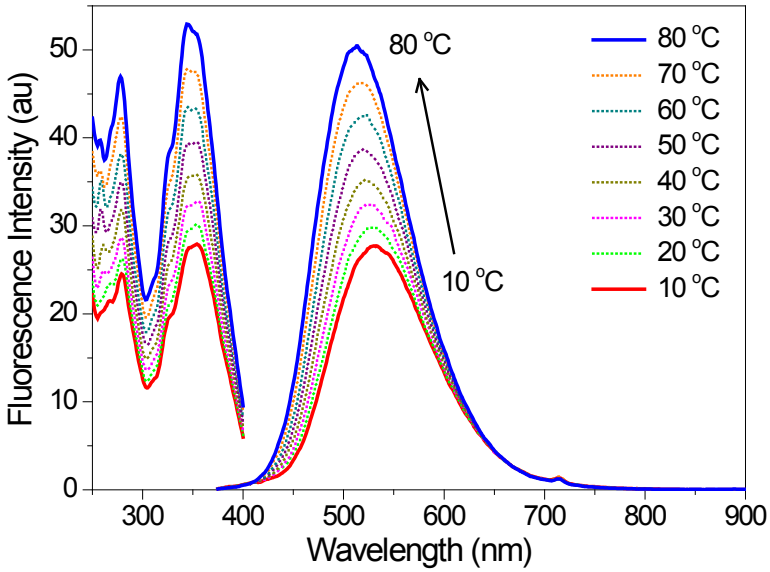

Figure S3. Temperature-dependent changes in the fluorescence emission and excitation spectra of the subcomponent **2** (10 μM) in acetonitrile, λ_{ex} = 357 nm. Excitation spectra were collected at the respective emission maxima.

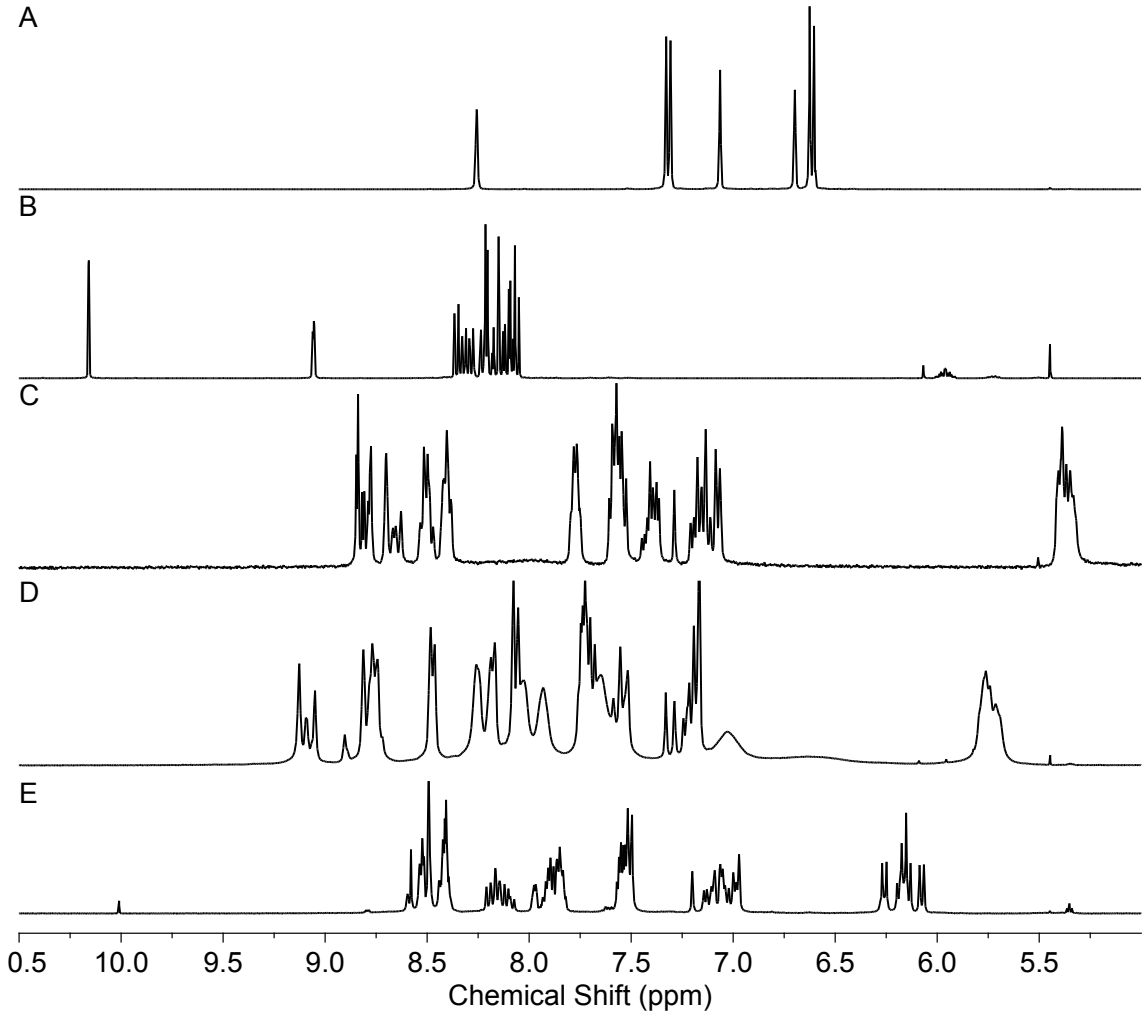

Figure S4. Partial ^{1}H NMR spectra of the subcomponents (A) **1** and (B) **2** and the cages (C) **4**, (D) **5**, (E) and **6** in CD_3CN.

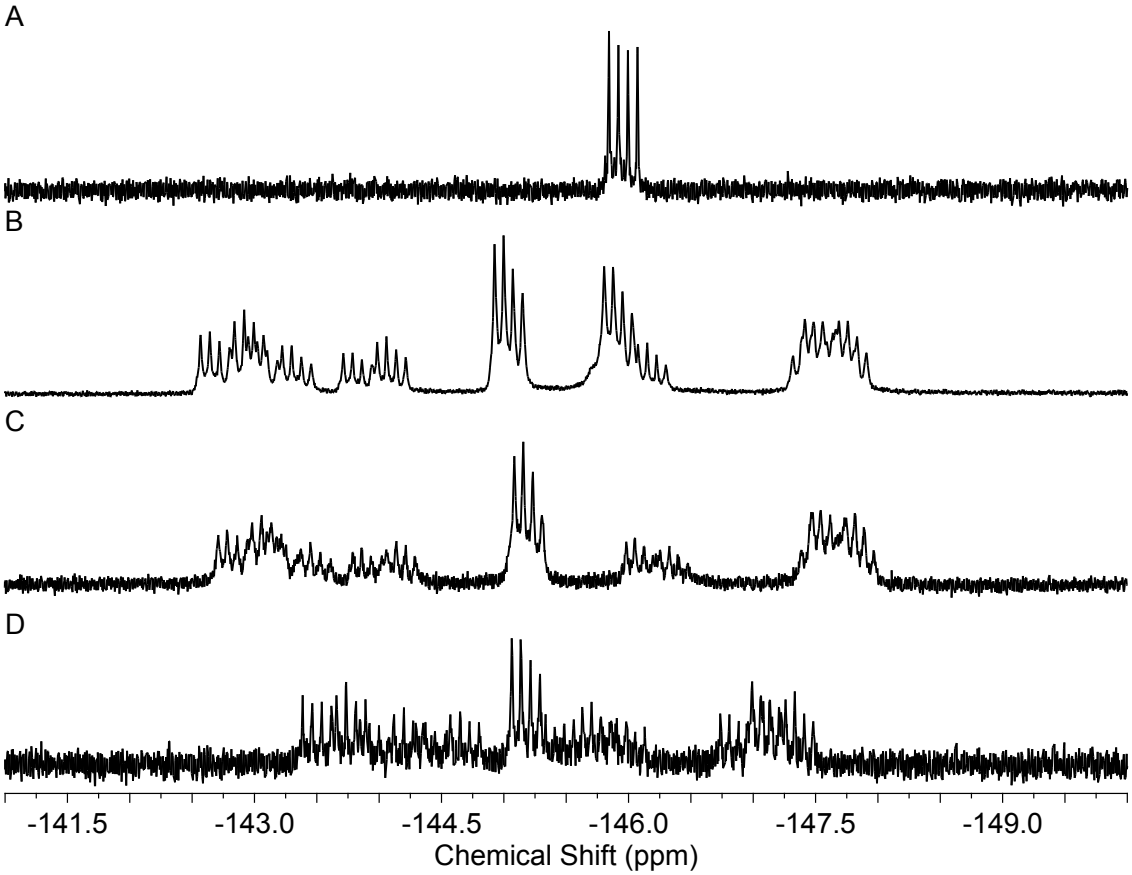

Figure S5. Partial ^{19}F NMR spectrum of the subcomponent (A) **1** and the cages (B) **4**, (C) **5**, and (D) **6** in CD_3CN.

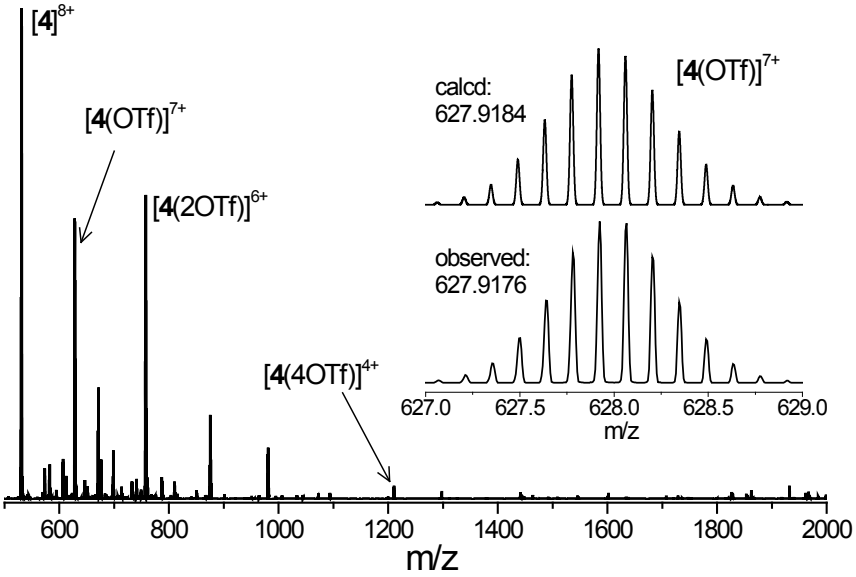

Figure S6. High-resolution mass spectrum of cage **4** along with the simulated and experimental isotopic distributions as inset.

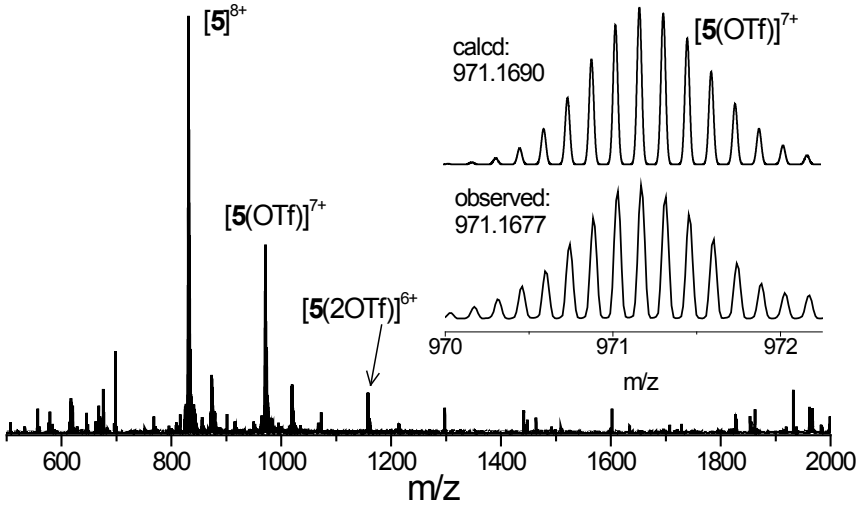

Figure S7. High-resolution mass spectrum of cage **5** along with the simulated and experimental isotopic distributions as inset.

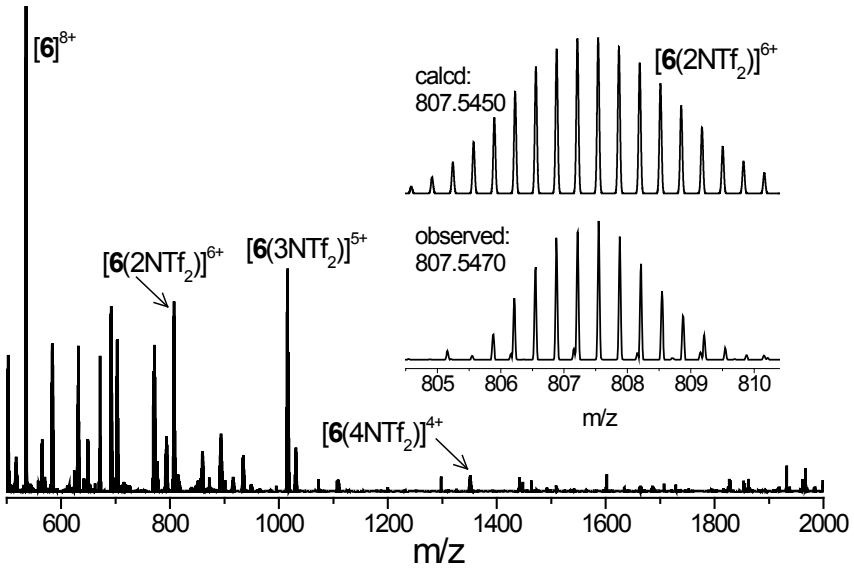

Figure S8. High-resolution mass spectrum of cage **6** along with the simulated and experimental isotopic distributions as inset.

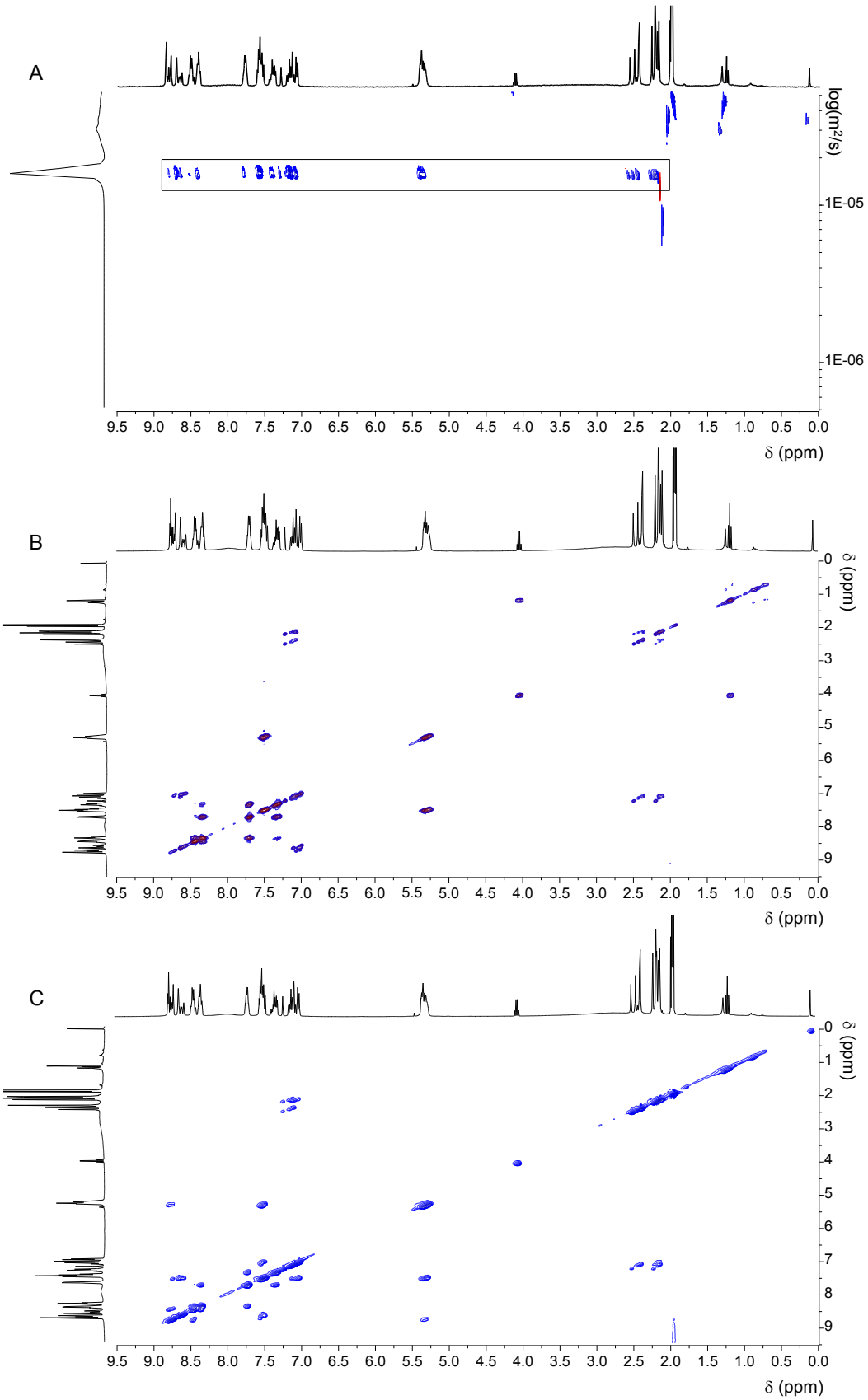

Figure S9. (A) DOSY, (B) ^{1}H-^{1}H COSY, and (C) NOESY spectra of cage **4** in CD_3CN.

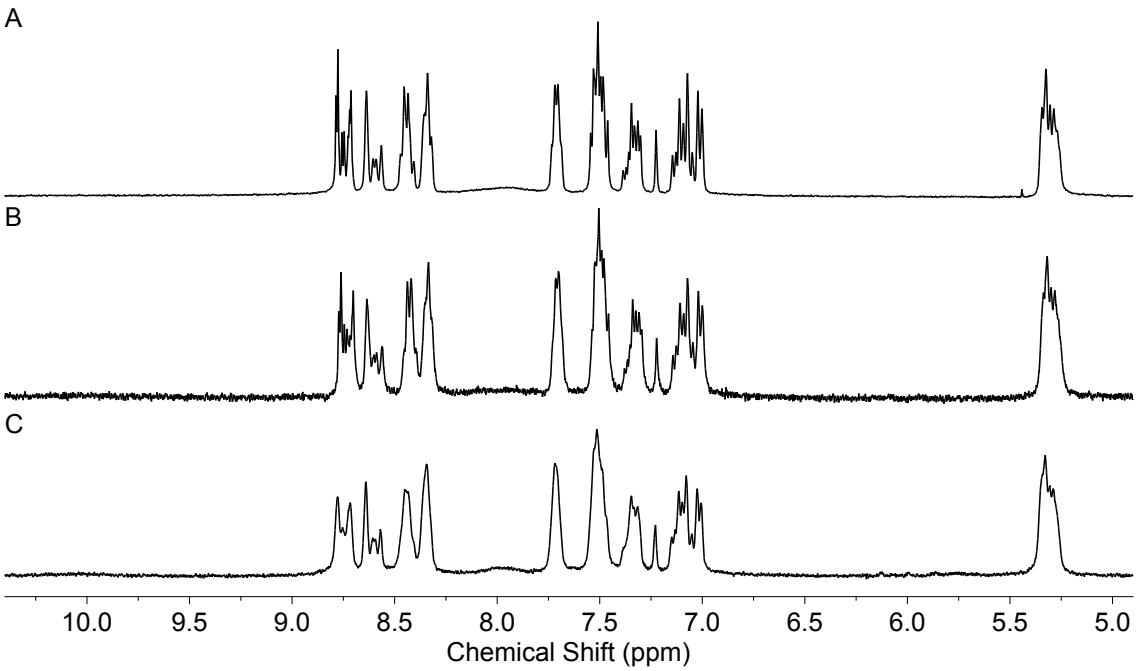

Figure S10. (A) Partial ^{1}H NMR spectrum of cage **4** (1 mM), and in the presence of 2 equivalents of tetrabutylammonium salts of (B) acetate and (C) azide in CD_3CN.

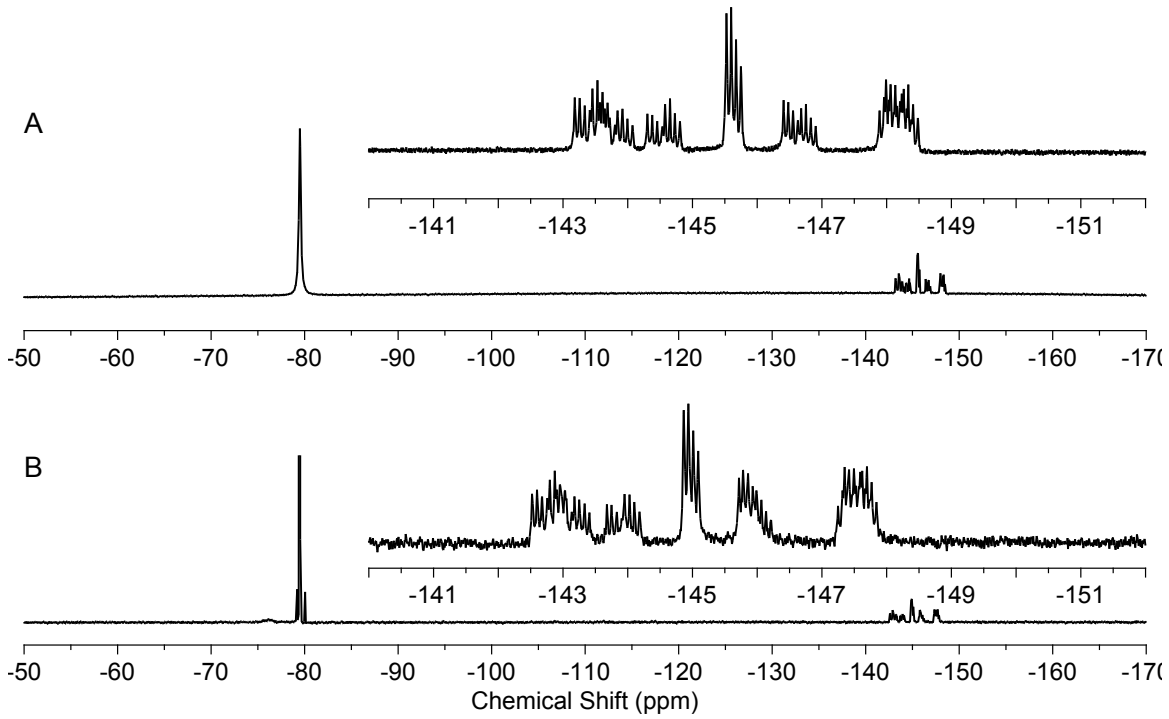

Figure S11. Partial ^{19}F NMR spectrum of the cage **4** (1 mM) (A) in the absence and (B) presence of 2 equivalents of tetrabutylammonium acetate in CD_3CN. Insets show the region between –140 to –150 ppm.

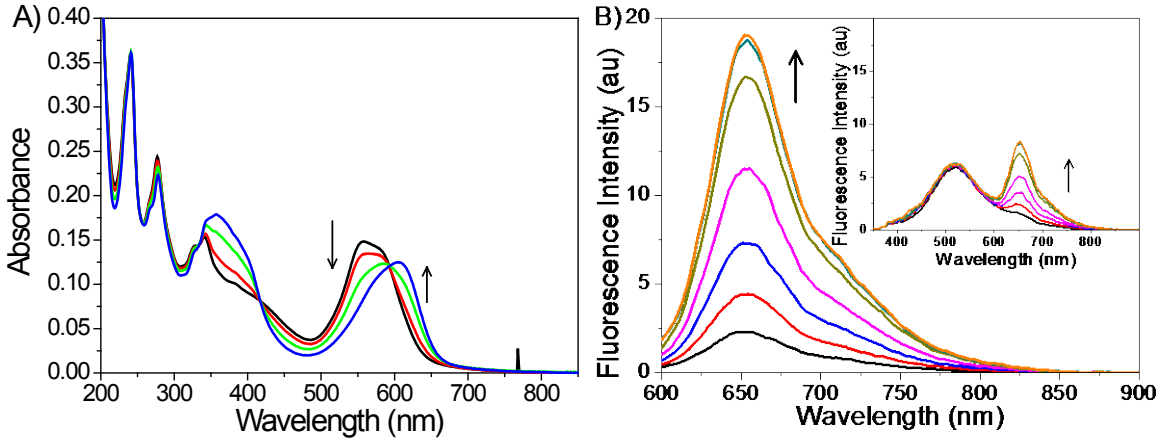

Figure S12. Changes in the (A) UV-Vis absorption and (B) fluorescence spectra (λ_{ex} = 590 nm) of **5** (110 nM) with the addition of tetrabutylammonium acetate (0→5.77 μM) in acetonitrile. Inset of (B) shows the corresponding fluorescence spectra excited at 333 nm.

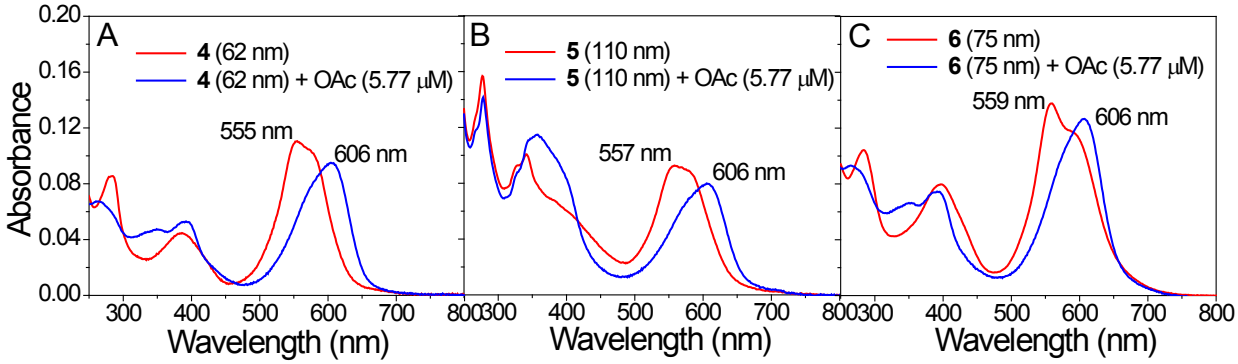

Figure S13. UV-Vis absorption spectra of cages (A) **4**, (B) **5**, and (C) **6** in the absence and presence of tetrabutylammonium acetate in acetonitrile.

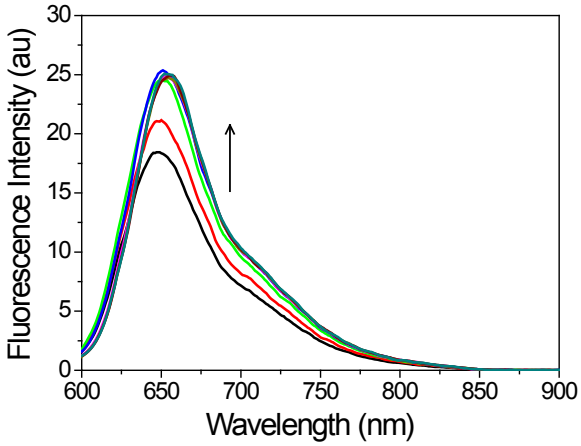

Figure S14. Changes in the fluorescence spectrum of cage **6** (75 nM) with the addition of tetrabutylammonium acetate (0→5.77 μM) in acetonitrile.

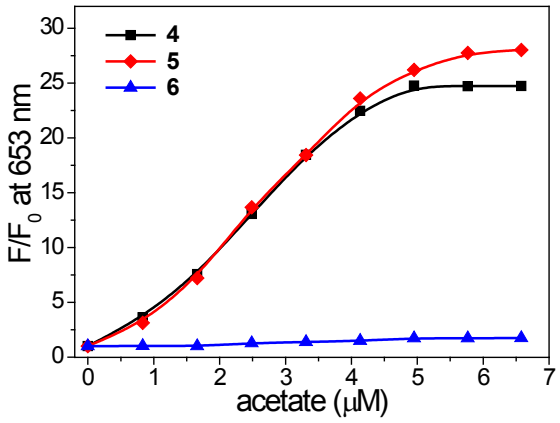

Figure S15. Relative changes in the fluorescence intensity of cages **4** (67 nm), **5** (110 nm), and **6** (75 nM) at 653 nm with the successive addition of tetrabutylammonium acetate (0-5.77 μM), λ_{ex} = 590 nm.

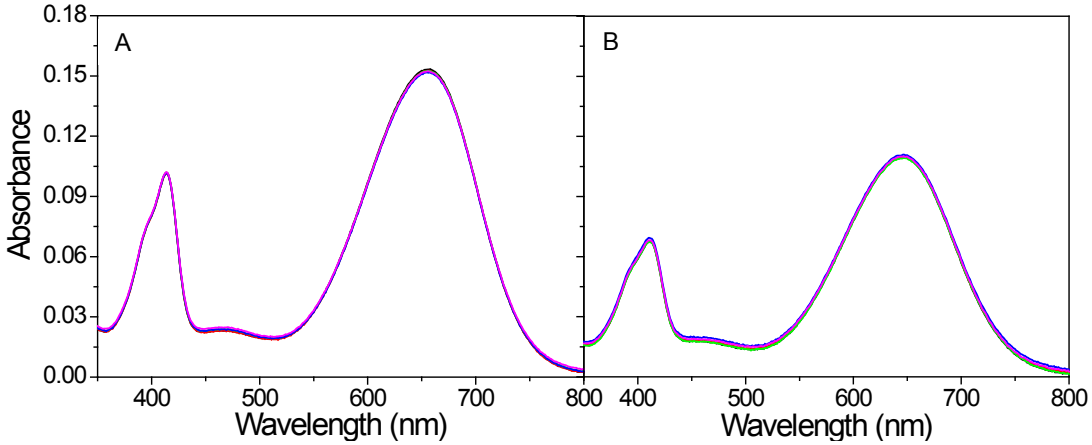

Figure S16. Changes in the UV-Vis absorption spectrum of **1** (3.5 μM) following the addition of (A) tetrabutylammonium acetate (0→5.77 μM) in acetonitrile and (B) L-cysteine (0-49.5 μM) in 50% acetonitrile-water mixture.

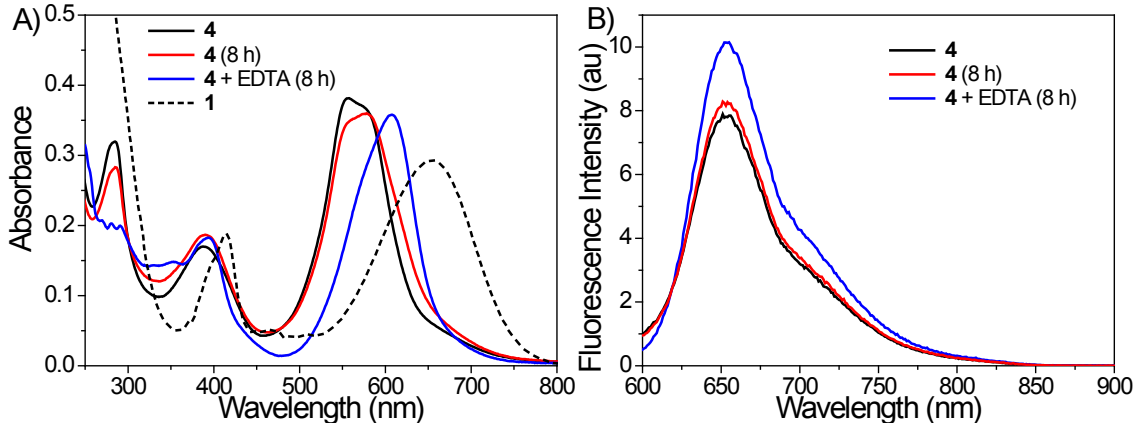

Figure S17. Time-dependent changes in the (A) UV-Vis absorption and (B) fluorescence spectra (λ_{ex} = 580 nm) of **4** (150 nM) in the absence and presence of EDTA in acetonitrile. As EDTA is not highly soluble in acetonitrile, it was added as solid to a solution of **4**. The resulting solution was filtered and used for optical measurements. For comparison, an absorption spectrum of **1** in acetonitrile is also shown in (A).

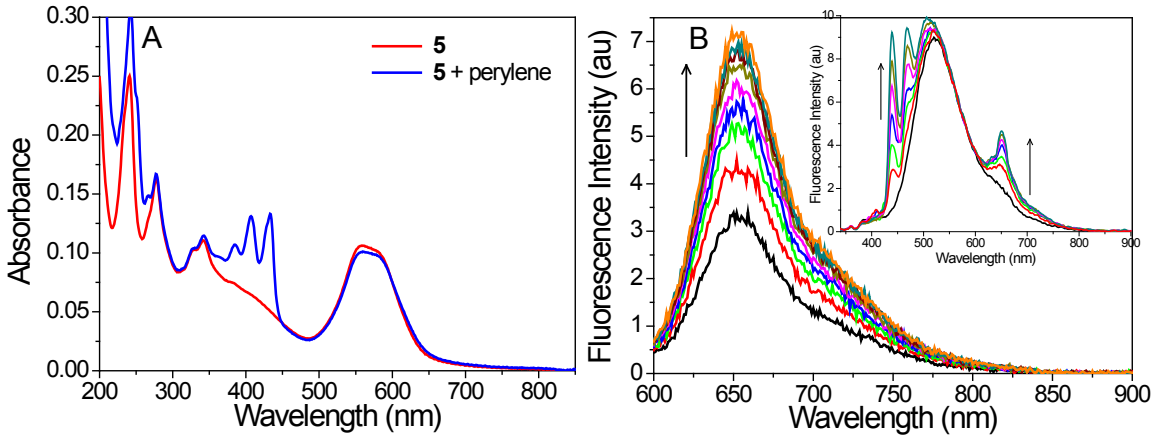

Figure S18. Changes in the (A) UV-Vis absorption and (B) fluorescence spectra of **5** (110 nM) following the addition of perylene (0→12.9 μM) in acetonitrile, λ_{ex} = 590 nm. Inset of (B) shows the corresponding spectra when excited at 333 nm.

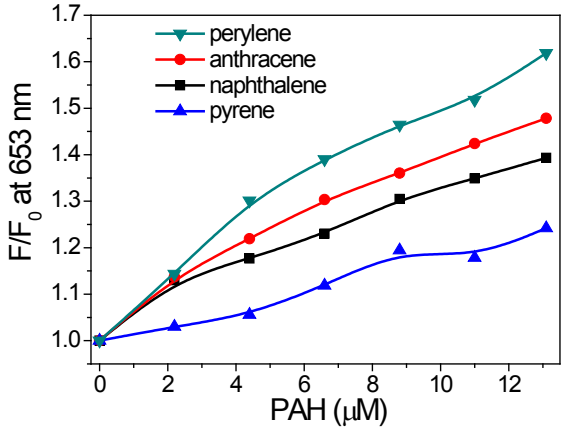

Figure S19. Relative changes in the fluorescence intensity of **5** (110 nM) at 653 nm with the addition of various polycyclic aromatic hydrocarbons (PAHs) in acetonitrile.

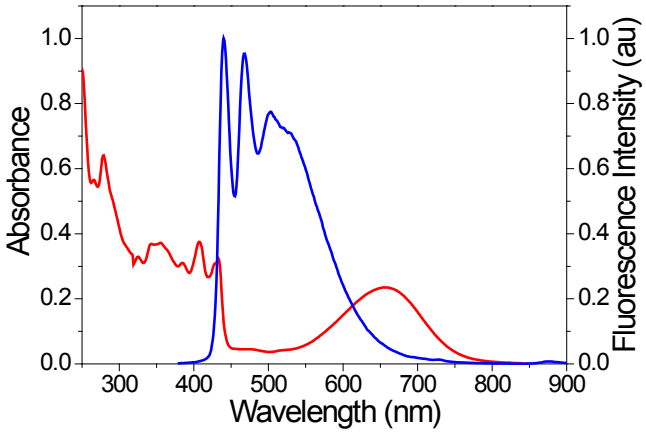

Figure S20. Absorption (red) and fluorescence spectra (blue) of a mixture of **1** (5.5 μM), **2** (11 μM) and perylene (16.6 μM) in acetonitrile, λ_{ex} = 365 nm.

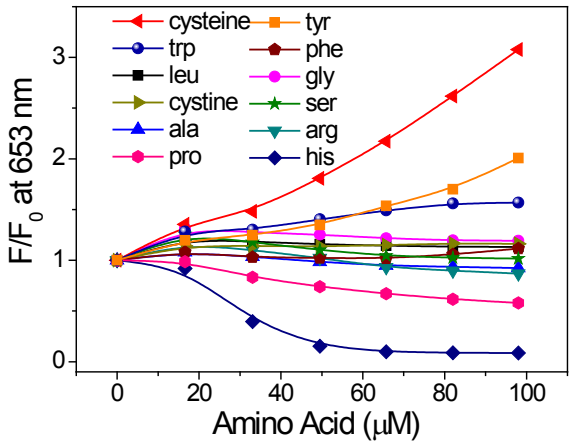

Figure S21. Relative changes in the fluorescence intensity of cage **4** (52 nM) at 653 nm with the addition of amino acids in 50% acetonitrile-water mixture.

References

1. J. K. Clegg, J. Cremers, A. J. Hogben, B. Breiner, M. M. J. Smulders, J. D. Thoburn and J. R. Nitschke, *Chem. Sci.*, 2013, **4**, 68-76.
2. R. F. Kubin and A. N. Fletcher, *J. Lumin.*, 1982, **27**, 455-462.
3. L. Yu, K. Muthukumaran, I. V. Sazanovich, C. Kirmaier, E. Hindin, J. R. Diers, P. D. Boyle, D. F. Bocian, D. Holten and J. S. Lindsey, *Inorg. Chem.*, 2003, **42**, 6629-6647.
4. H. L. Kee, C. Kirmaier, L. Yu, P. Thamyongkit, W. J. Youngblood, M. E. Calder, L. Ramos, B. C. Noll, D. F. Bocian, W. R. Scheidt, R. R. Birge, J. S. Lindsey and D. Holten, *J. Phys. Chem. B*, 2005, **109**, 20433-20443.
5. Y. Hayashi, S. Yamaguchi, W. Y. Cha, D. Kim and H. Shinokubo, *Org. Lett.*, 2011, **13**, 2992-2995.